**Jian-Lian Chen**
**Kai-Hsin Hsieh**

School of Pharmacy, China Medical University, Taichung, Taiwan

Received June 26, 2010
Revised August 27, 2010
Accepted August 27, 2010

Research Article

# Polyacrylamide grafted on multi-walled carbon nanotubes for open-tubular capillary electrochromatography: Comparison with silica hydride and polyacrylate phase matrices

A new nanoparticle-bound polymer stationary phase was prepared by *in situ* polymerization of methacrylamide (MAA), bis-acrylamide crosslinker, and carboxylated multi-walled carbon nanotubes (multi-walled CNTs; MWNTs), using the abundant double bonds in the cyclopentadienyl rings in MWNT structure, on a silanized capillary. Each intermediate capillary between the synthesis steps was characterized by SEM, by ATR-IR, and by EOF measurements varying the pH, concentration, and volumetric ratios of ACN in running buffers. The resulting EOF profile was comparable to those of two other capillaries with different phase matrices, silica hydride and polybutyl methacrylate (BMA) phases. With the complex functionality of MWNTs on the hydrophilic polyacrylamide network, the MAA-CNT capillary was capable of separating diverse samples with a wide range of polarity and dissociation properties using open-tubular CEC. Besides optimizing CEC conditions, the migration times of samples were analyzed with respect to velocity and retention factors to evaluate electrophoretic and chromatographic contributions to the CEC mechanism. The migration rates of benzoic acids were determined by the electrophoretic mobilities of the various phenolate ions, while phenolic aldehydes and ketones were additionally influenced by chromatographic interactions, such as π–π, electrostatic effects, hydrogen bonding, and hydrophobic interactions. The retention factors were greater for flavonoids, which are polyphenolic, than for simple phenols, but were smaller than those obtained from the hydrophobic BMA-CNT column. A complete well-resolved separation of the cationic forms of tetracyclines was acheived either by electrophoresis or by chromatography in the MAA-CNT capillary, but not in the BMA-CNT and silica hydride-CNT capillaries.

**Keywords:**
CEC / Carbon nanotubes / Open-tubular / Polyacrylamide / Stationary phases
DOI 10.1002/elps.201000339

## 1 Introduction

Since one does not have to fabricate frits as with particulate-packed columns, or to blend monomeric reagents with suitable porogens in precise proportions as with monolithic columns, the open-tubular (OT) format is a comparatively straightforward method of column preparation for CEC [1, 2]. Although open-tubular CEC (OT-CEC) suffers from a low phase ratio, some strategies to increase the loadability of the designed ligands were adopted, such as etching the capillary wall, stacking with multilayers, or coating with porous polymeric layers [3–5]. *In situ* polymerization of functional monomers can directly produce the porous-layered phases chemically bonded on an OT column with a longer lifetime and better reproducibility than capillaries with physical coatings. In contrast to monoliths, it is easy to leave a certain thickness of polymer film on a capillary wall for initial studies of new stationary phases. In this manner, some research has shown the separation of various analytes on the styrene-based [6, 7] and acrylate-based [8–16] OT-CEC columns. To our knowledge, the acrylamide-based phases have not been applied in the OT-CEC, but have been extensively studied in the monolithic format [17].

**Correspondence:** Dr. Jian-Lian Chen, School of Pharmacy, China Medical University, No.91 Hsueh-Shih Road, Taichung 40402, Taiwan
**E-mail:** cjl@mail.cmu.edu.tw
**Fax:** +886-4-22031075

**Abbreviations:** **BMA,** butylmethacrylate; **CNT,** carbon nanotube; **CTC,** chlortetracycline; **MAA,** methacrylamide **γ-MAPS,** 3-(trimethoxysilyl) propylmethacrylate; **MNC,** minocycline; **MWNT,** multi-walled carbon nanotube; **OT,** open tubular; **PLOT,** porous-layered open-tubular; **TCs,** tetracyclines

 

Nanoparticles exhibiting favorable surface-to-volume ratios would also create efficient stationary phases of electrochromatography [18]. However, only a few of the nanomaterials, including silica [19], titanium oxide [20, 21], gold [22, 23], and carbon nanotubes (CNT) [24–26], had been chemically bonded in the OT-CEC phases. The multi-walled carbon nanotubes (MWNTs) were incorporated after the silanization and coupling with glutaraldehyde on the inner surface by Sombra *et al.* [24]. In a previous work, we utilized the double bonds within the MWNTs structure as a functional handle to covalently attach the nano moieties onto the silica hydride (SiH) phase creating a stable Si–C linkage and forming a SiH-CNT capillary [25]. Moreover, the MWNTs-bound polybutyl methacrylate phase, BMA-CNT, in an OT fashion was successfully synthesized [26], as the π-bonds in the cyclopentadienyl carbons at the curved parts of the CNTs are assumed to be involved in the polymerization reaction with methyl methacrylate [27, 28].

Particle-bound polymer phases represent a new type of hybrid OT-CEC column, which combines a variety of advantages of rich in nanoparticles-loading capacity, high permeability of porous polymer film, and easy in fabricating OT columns. The polymer material used in the hybrid phase will relate to the adhesion extent of particulates, surface chemistry, and phase morphology. In comparison with acrylate- and styrene-based phases, which most recent studies were focused on their development and application in reversed-phase mechanism, acrylamide-based phases showed some hydrophilic characters in monolithic HPLC and CEC [29–31].

In this study, the carboxylated multi-walled CNT were copolymerized with methacrylamide (MAA) monomer and bis-acrylamide crosslinker to develop a particle-bound porous-layered open-tubular capillary. The complete MAA-CNT capillary was characterized by SEM and ATR-IR. Furthermore, the effect on electroosmotic mobilities ($\mu_{eo}$) caused by changes in pH, buffer concentration, and the volumetric addition of ACN to the running buffers were recorded, tracked for each intermediate capillary between the synthesis steps, and compared with the SiH-CNT and BMA-CNT capillaries. The MAA-CNT column was used to separate a number of benzene derivatives, flavonoids, and tetracyclines (TCs) as these test samples cover a wide range of $pK_a$ and polarity values. These separations also allowed us to assess the relative electrophoretic and chromatographic contributions to the CEC mechanism, as well as the suitability to different phase matrices.

## 2 Materials and methods

### 2.1 Reagents and chemicals

Most chemicals used were of analytical or chromatographic grade. Purified water (18 MΩ cm) from a Milli-Q water purification system (Millipore, Bedford, MA, USA) was used to prepare samples and buffer solutions. All solvents and solutions for CEC analysis were filtered through a 0.45-μm cellulose ester membrane (Adventec MFS, Pleasanton, CA, USA).

#### 2.1.1 Reagents

MAA, Bis, ammonium persulfate, 2,2-diphenyl-1-picrylhydrazyl, TEMED, sodium tetraborate, phosphoric acid, hydrochloric acid, ACN, and DMSO were purchased from SigmaAldrich (Milwaukee, WI, USA). Boric acid, tri-sodium phosphate, methanol, acetone, and ethanol were obtained from Panreac (Barcelona, Spain). Nitric acid, sodium hydroxide, sodium dihydrogenphosphate, disodium hydrogenphosphate, tri-sodium phosphate, citric acid, sodium dihydrogen citrate, and trisodium citrate were supplied by Merck KGaA (Garmstadt, Germany). 3-(Trimethoxysilyl) propylmethacrylate (γ-MAPS), sodium acetate, and tris(hydroxymethyl)aminomethane were received from J. T. Baker (Phillipsburg, NJ, USA), TEDIA (Fairfield, OH, USA) and Acros (Thermo Fisher Scientific, Geel, Belgium). The MWNTs were supplied by Conyuan Biochemical Technology (Taipei, Taiwan) and their specifications are: 20–40 nm external diameter; 5–15 um length; 95–98% purity, by volume; 40–300 $m^2/g$ for special surface area; 2 wt% amorphous carbon; and 0.2 wt % of ash.

#### 2.1.2 Analytes

Three groups of test samples are benzene derivatives, flavonoids, and TCs, and their chemical structures are illustrated in Fig. 1. 4′-Hydroxy-3-methoxyacetophenone (acetovanillone), 3,5-dimethoxy-4-hydroxybenzaldehyde (syringylaldehyde), quercetin, catechin, hesperetin, daidzein, epicatechin, hesperidin, naringenin, naringin, 5-methoxyflavone, minocycline (MNC), C, oxytetracycline, doxycycline, and meclocycline were purchased from Sigma-Aldrich. 4-Hydroxy-3-methoxybenzoic acid (vanillic acid), 4-hydroxy-3,5-dimethoxybenzoic acid (syringic acid), 3,5-dimethoxy-4-hydroxyacetophenone (acetosyringone), 4-nitrobenzoic acid, and methacycline were received from Acros (Thermo Fisher Scientific). Chlortetracycline (CTC) was obtained from Fluka (Sigma-Aldrich). 4-Hydroxyacetophenone, 4-hydroxybenzoic acid, benzoic acid, and benzamide were supplied by Merck KGaA. 4-Hydroxy-3-methoxybenzaldehyde (Vanillin) and 4-hydroxybenzaldehyde were supplied by Lancaster (Morecambe, England). Stock solutions of samples were prepared in 0.1 M in ACN/$H_2O$ (1/2, v/v) for benzene derivatives, 0.25 mg/mL in MeOH for flavonoids, and 2 mg/mL in MeOH for TCs. The test samples were collected from stock solutions with equal volume except for 4-hydroxyacetophenone and 4-hydroxybenzaldehyde with double volume, and for benzoic acid and tetracycline with triple volume.

### 2.2 Instrumentation

The laboratory-built electrophoresis apparatus consisted of a ±30 kV high-voltage power supply (TriSep TM-2100,

 

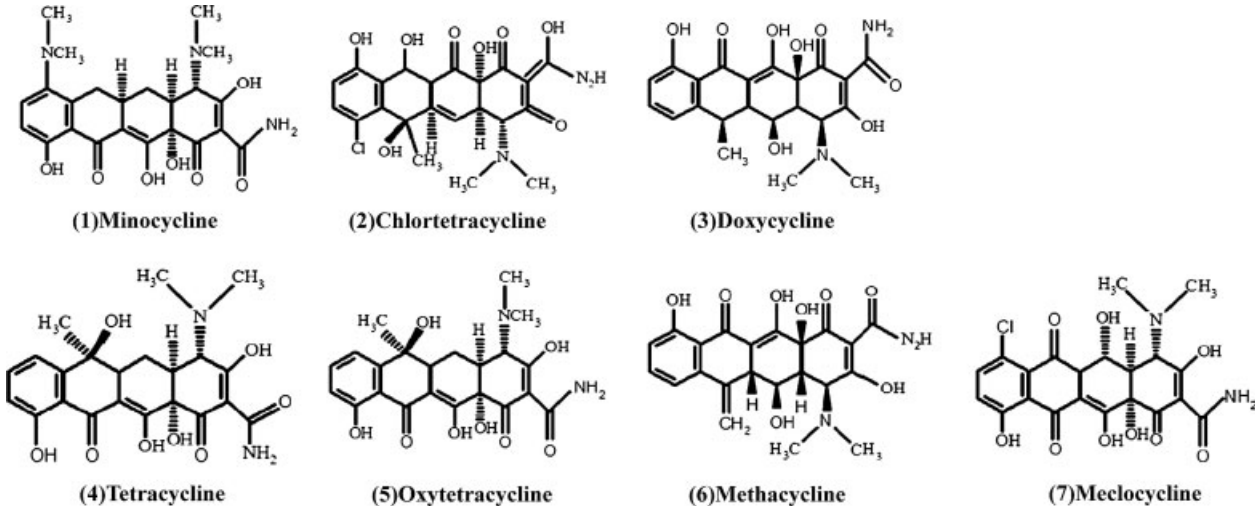


**Figure 1.** Chemical structures of seven TCs. The numbers in the parentheses indicate the migration order used for the electrochromatograms of Fig. 8.

Unimicro Technologies, CA, USA) and a UV–Vis detector (LCD 2083.2 CE, ECOM, Prague, Czech). Electrochromatograms were recorded using a Peak-ABC Chromatography Data Handling System (Kingtech Scientific, Taiwan). A Joel JSM-6700F Scanning Microscopy at the National Chung Hsing University acquired the SEM images at an accelerating voltage of 3.0 kV. The ATR-IR spectra were obtained by a Shimadzu Prestige-21 IR spectrometer, equipped with a single reflection horizontal ATR accessory (MIRacle, PIKE Technologies, WI, USA).

### 2.3 Preparation of capillary columns

A new, bare capillary column (Polymicro Technologies, Phoenix, AZ, USA) with 375 μm od × 75 μm id was treated with 1.0 M NaOH and successively washed with pure water, 0.1 M HCl, pure water, and acetone. The clean, bare capillary was then filled with a solution of 2,2-diphenyl-1-picryl-hydrazyl (0.02 g), γ-MAPS (1.0 mL), and MeOH (1.0 mL) and was kept at room temperature for 24 h to complete silanization. Following a series of rinses with MeOH, $H_2O$, and acetone, the resulting silanized capillary was filled with a polymerization solution, which contained MAA (0.03 mol), Bis-acrylamide (0.01 mol), acid-treated MWNTs (30 mg), TEMED (0.15 mL, 5% v/v), ammonium persulfate (0.3 mL, 10% w/v), and borate buffer (30 mL, pH 8.1, 150 mM). The acid-treated MWNTs were obtained by first refluxing the MWNTs in $HNO_3$ (3.0 M) for 24 h at 60°C, then in HCl (5.0 M) for 6 h at 120°C. Most of the mixed solution was purged out of capillary by blowing nitrogen through the tube at 40 psi for 5 min, leaving the capillary wall with a thin layer of solution ready to react with the silanized capillary. After the purge, the capillaries stood at room temperature for 30 min to complete the polymerization reaction. Finally, the completed MAA-CNT capillaries were washed successively with $H_2O$, ethanol, and acetone for 30 min and were then prepared for the next CEC testing.

The synthesis procedures for fabricating the SiH-CNT2 capillary, which acid-treated MWNTs were bonded on a silica-hydride molecular phase, and fabricating the BMA-CNT capillary, which acid-treated MWNTs were *in situ* copolymerized with butyl methacrylate (BMA) and ethylene dimethacrylate crosslinker, were introduced in detail in the previous papers, respectively [25, 26].

### 2.4 CEC conditions

Most experiments were conducted using common CZE buffers, namely Tris, sodium acetate, sodium citrate, sodium phosphate, ammonium carbonate, and sodium borate at a pH range of 8.5–10.5 and an ionic concentration range of 10–100 mM. DMSO was used as the neutral marker. At the end of the analysis, the studied capillary was washed with methanol, pure water, and running buffer, sequentially, during the intervals between runs. Prior to a sample injection, a working voltage was applied for 5 min to condition the charge distribution in the column. The prepared test samples were introduced by siphoning using a height difference and the samples were detected by UV light absorption measurements at 214 nm for DMSO, 214 nm for benzene derivatives, 280 nm for flavonoids, and 355 nm for TCs.

## 3 Results and discussion

### 3.1 Characterization of MAA-CNT phase

#### 3.1.1 ATR-IR spectrum and SEM image

The ATR-IR spectra of the finely ground powder of the MWNT materials, the MAA-CNT bulk material, and the

 

MAA-CNT capillaries are shown in Figs. 2(A–C), respectively. These substances show the characteristic absorption of CNT at 1520 $cm^{-1}$ for conjugated C = C stretching [32], 1640 $cm^{-1}$ for the non-conjugated C = C stretching [33], 1700 $cm^{-1}$ for C = O stretching [24, 33] and ~3500 $cm^{-1}$ for –OH stretching [34] from the carboxyl groups introduced by the $HNO_3$/HCl treatment of MWNTs. The carboxyl group has been reported to be the primary product of nitric acid oxidation of CNT [35], although other oxygen-containing functional groups have been reported as products in the oxidation of some carbon materials [36].

Owing to the graft polymerization of MAA onto MWNTs, the spectrum of Fig. 2(B) shows the characteristic absorption at 1000~1350 $cm^{-1}$ for C–N stretching and 3100–3500 $cm^{-1}$ for N–H stretching [32]. Figure 2(D) presents the SEM image of the newly synthesized polymer composite, showing that the polyMAA was obviously attached to the MWNT backbone. Through the *in situ* polymerization process, the new composite was formed and coated on the silanized capillary to construct the MAA-CNT capillary. After the attachment, the Si–O stretch corresponding to the capillary material appeared at 1100 $cm^{-1}$ as shown in Fig. 2(C).

### 3.1.2 The EOF profiles upon buffer pH

Before applying the MAA-CNT capillary to electochromatographic analyses, the characterization of the EOF driven by the capillary in different media is necessary. Some of the chemical properties of the MAA-CNT phase could also be revealed by these measurements. The curves shown in Fig. 3 illustrate the dependence of $\mu_{eo}$ on the pH levels of the phosphate buffer for the six capillaries, including the bare fused-silica capillary, the γ-MAPS silanization capillary, the MAA-CNT capillary, the silica-hydride-modified capillary, SiH-CNT2, from which we cited data from the previous study [25], and the BMA-CNT capillary from the study [26].

From the graphs, we see that the γ-MAPS capillary has a similar response as the bare capillary but with a decreased $\mu_{eo}$ value. The near 20% decrease could be interpreted as a correlate to the degree of silanization if the bonded γ-MAPS molecules are assumed not to be further dissociated. That is, nearly 80% of silanol groups would be left unreacted on the capillary wall. The unreacted silanols seem to be shielded by the polymerization and do not affect the EOF performance of the MAA, MAA-CNT, BMA-CNT capillaries, since the $\mu_{eo}$ values of the polymer capillaries do not have an obviously steep increase beginning near pH 6.8 as with the bare and the γ-MAPS capillaries.

The difference in the synthesis of the wall coatings between the two MAA polymerization capillaries is whether the MWNTs were added into the monomeric solution or not. Without the addition of MWNTs, the fixed phase of the MAA capillary was composed of MAA with bis-acrylamide added for crosslinking. The acrylamide-based polymer contains very weakly basic amide units, which p$K_a$ value is about the same as that of acetamide, p$K_a$ = 17 [37]. No peak of neutral marker showing within a 2h run indicates that the MAA phase surface was nearly uncharged over the studied pH range. This result was accordant with other polyacrylamide phases without crosslinking and thus confirmed the completion of polymerization throughout the capillary [38, 39].

In contrast with the MAA capillary, the MAA-CNT capillary, which incorporated MWNTs into the polyacrylamide network, raised the $\mu_{eo}$ values. A similar EOF pattern could also be found with the BMA-CNT phase and

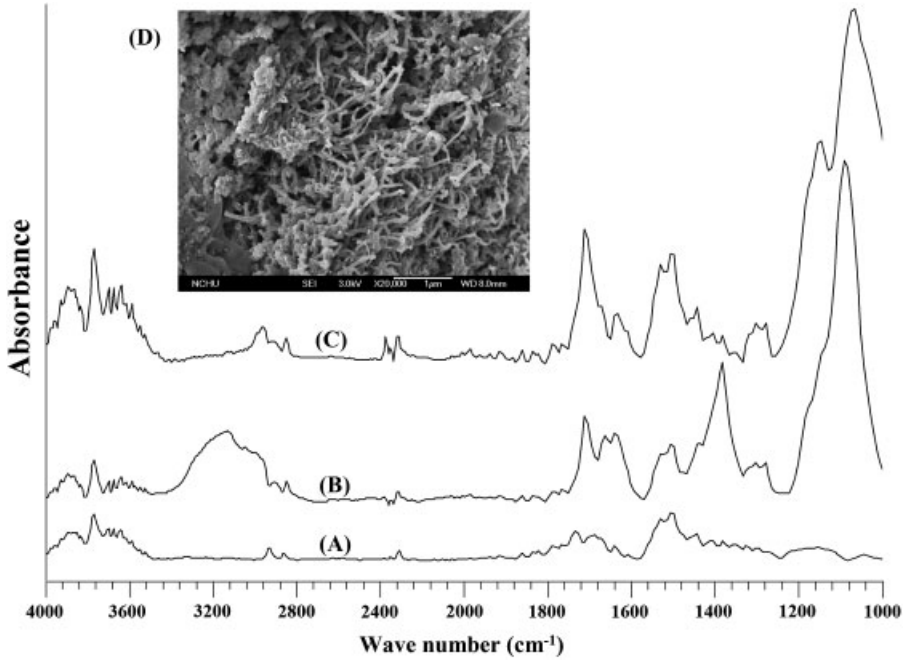


**Figure 2.** ATR-IR spectra of (A) acid-treated multi-walled CNT; (B) MAA-CNT powder; and (C) MAA-CNT capillary. (D) SEM image of the MAA-CNT composite at 20 000 magnifications. The voltage used was 3.0 kV.

 

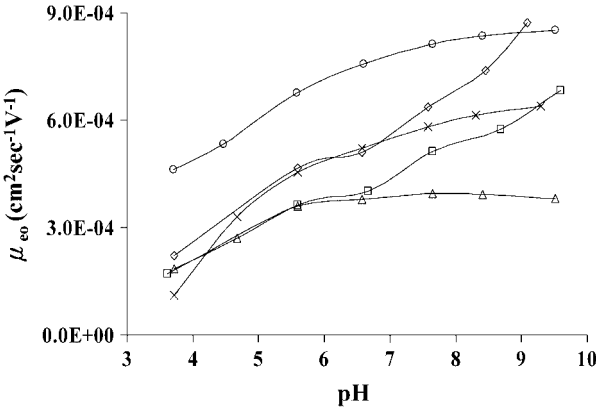


**Figure 3.** Dependence of electroosmotic mobility on buffer pH. Columns: (◇) a bare fused-silica capillary; (□) a γ-MAPS-silanized capillary; (△) the MAA-CNT capillary; (x) the SiH-CNT2 capillary; (○) the BMA-CNT capillary. Conditions: BGE, phosphate buffer, 50 mM; sample, DMSO; hydrostatic injection, 10 cm, 1 sec; applied voltage, 10 kV; detection, 214 nm. The data on the bare fused-silica, γ-MAPS-silanized, SiH-CNT2, and BMA-CNT capillaries are collected from the previous reports [16, 25, 26].

the polyacrylamide-based phase having sulfonate functionality [26, 40]. The MWNTs used here were sequentially pretreated with nitric and hydrochloric acids before incorporation. It is supposed that oxidation occurred and that carboxylate groups were intentionally introduced to the $HNO_3$-treated MWNT macromolecules. Any metal ions, which might be derived from the catalyst used for the synthesis of the MWNTs and could reduce the negative charge density on the Stern layer and slow a cathodic EOF, were removed by refluxing in HCl [41]. Thus, compared with the MAA capillary, the phase surface of the MAA-CNT capillary possesses many more anionic groups and generates strong cathodic EOF Furthermore, an apparent increase in the $\mu_{eo}$ values could be found in the pH 3.5–5.5 range, which correlates well to the acid dissociation constants of most carboxylic acids, and a maximum is reached at higher pH levels, where the dissociation of carboxylic groups should be completed. Based on the same acid dissociation, the shapes of the curves of the SiH-CNT2 and BMA-CNT capillaries are similar to that of the MAA-CNT capillary. The $\mu_{eo}$ maximum observed at higher pH levels in the MAA-CNT capillary was lower than those in the SiH-CNT2 and BMA-CNT capillaries. The reason could be that more of MWNTs were embedded in the MAA phase matrix as the hydrophilic MAA monomers had a greater affinity to carboxylated MWNTs and a higher coverage of polymer materials wrapped around the MWNTs after polymerization. Such a problem did not occur with the SiH-CNT2, although the SiH-CNT2 had fewer bonded MWNTs than the MAA-CNT and BMA-CNT capillaries.

The reproducibility of capillary fabrication was evaluated from the $\mu_{eo}$ values measured at pH 7.6 for five runs in a MAA-CNT capillary using the same format. The mean and RSD values were ($4.13 \times 10^{-4}\,cm^2\ V^{-1}\,S^{-1}$ $mM^{-1}$, 3.2%), ($3.90 \times 10^{-4}\,cm^2\,V^{-1}\,S^{-1}\,mM^{-1}$, 3.8%), and ($3.79 \times 10^{-4}\,cm^2\,V^{-1}\,S^{-1}\,mM^{-1}$, 4.7%) for three replicate capillaries. At the 95% confidence level, no significant difference in $\mu_{eo}$ values between columns was observed by *t*-test. This indicated that the fabrication of the MAA-CNT capillaries was pretty robust.

### 3.1.3 The EOF profiles upon the ionic strength and the ratio of ACN modifier

In open tubes with thin double layers, which thickness (~ 30 Å at 10 mM buffer) is far less than the capillary radius, the EOF mobility, $\mu_{eo}$, can be expressed by the Smoluchowski equation [42, 43]:

$$\mu_{eo} = \varepsilon\varepsilon_o\zeta/\eta \quad (1)$$

where ε is the dielectric constant of the medium, $\varepsilon_o$ is the permittivity of the vacuum, η is the viscosity of the bulk solution, and ζ is the zeta potential at the capillary inner wall. When the surface charge is independent of the electrolyte concentration and exp $(ze\psi_o/k_BT) \gg 1$

$$\psi_o = (k_BT/ze)\ \log\ C + \text{Constant} \quad (2)$$

where $\psi_o$ is the surface potential, $k_B$ is the Boltzmann constant, $T$ is the absolute temperature, and $e$ is the elementary charge [44]. Since the ζ potential is of the same order as the surface potential, the above equation can be rewritten to relate the EOF mobility to the buffer concentration as follows [45]:

$$\mu_{eo} = \varepsilon\varepsilon_o\zeta/\eta \approx -(\varepsilon\varepsilon_o k_BT/\eta ze)\ \log\ C + \text{Constant} \quad (3)$$

According to Eq. (3), the dependence of the EOF mobility on the logarithmic electrolyte concentration is linear.

The curve trend of $\mu_{eo}$ values along with the log $C$ axis is shown in Fig. 4(A). For the γ-MAPS-silanized and MAA-CNT columns, however, some points at lower concentrations were not on the line. This phenomenon could be explained by surface conductance and double-layer overlap [45, 46]. Surface conduction takes place in double layers containing the local presence of excess counter charges that may move under the influence of electric fields applied tangentially to the surface. It is the excess conduction that can be found from the total conductivity of a disperse system minus the same in the absence of a double layer and from some systems, which computed zeta-potentials depend in a bizarre way on the electrolyte concentration unless the interpretation of the experiments is improved to take account of it. A typical example, as shown in Fig. 4(A), is that the apparent mobility as a function of concentration sometimes passes through a maximum [46].

*As regards the* double-layer overlap, which is significant only when the channel diameter to the double-layer thickness ratio is smaller than 10, the double-layer thickness calculated for the present case is 30 Å at 10 mM and the occurrence of double-layer overlap can be excluded.

In the range from 30 to 100 mM, the curve for the γ-MAPS-silanized was linear ($R^2 = 0.9633$,

 

slope = $-6.0 \times 10^{-4}$ cm$^2$ V$^{-1}$ S$^{-1}$ mM$^{-1}$), while those for the MAA-CNT capillary were (0.9845, −7.4). The slope value of $-7.4 \times 10^{-4}$ is far from the estimated value, $-2 \times 10^{-4}$ [44], but is somewhat smaller than the slope value, $-8.2 \times 10^{-4}$, for the polyacrylate phase in the same porous-layered open-tubular format [16]. The two slopes were significantly greater than those obtained with packed capillary columns [47, 48] and this may be taken as a manifestation of the ''openness'' of the column [49]. The data for the γ-MAPS-silanized column and for the bare fused-silica one (0.9382, −3.3) are cited from the previous study [16]. In any case, the three curves in Fig. 4(A) were significantly different from those obtained with the particulate-packed capillary columns, which showed plateaus at high buffer concentrations [45]. Obviously, the linearity of these curves was not altered by Joule heating, which easily occurs at high buffer concentrations and in cases of monolithic and packed CEC columns [50].

The effect of ACN in the buffer solution on the $\mu_{eo}$ values is highlighted in Fig 4(B), which shows concave curves having a minimum around 40–60% ACN content. This profile is seen in various OT-CEC formats, such as direct polymer coating, stepwise fabrication, and *in situ* polymerization [16, 51–53], and is primarily the result of a change in the ratio of the dielectric constant to the viscosity of the running buffer with increasing ACN proportions from 0 to 100% (see the $Y_2$ axis in Fig. 4(B)). This situation suggests that the DMSO solute was a good EOF probe and that its chromatographic interaction with the modified phases could be ignored.

### 3.2 Separation of benzene derivatives

A mixture of 12 benzene derivatives, which 9 of them were oxidized phenolics and were often found in dissolved organic matter [54, 55], were used as probes to assess the CEC separation performance of the MAA-CNT capillary. The samples are possessed of benzene ring and diverse polarity with aldehydic, ketonic or acidic groups in expection of the π–π and polar–polar interactions with the MAA-CNT phase, which is characterized by the hybrid functionality of the conjugated double bonds on the carboxylated MWNTs and the hydrophilic polyacrylamide matrix. After trying several of the buffers listed in Section 2.4, the best peak shape and resolution was achieved with a borate-based buffer system. The electropherograms shown in Fig. 5 resulted from the borate running buffer at a fixed molarity (50 mM), but across different pH values (pH = 7.5, 8.6, and 9.5). Figure 5(B) demonstrated buffer at pH 8.6 created more selectivity than did either pH 7.5 or 9.5. Changing the buffer concentration to 30 and 100 mM verified the suitability of using the 50 mM concentration.

Comparison between the pseudo-effective electrophoretic mobility, $\mu_{ps}$, and the electrophoretic mobility, $\mu_{ep}$, is a fast screening method for the identification of chromatographic retention in the modified phases. The two values are easily calculated from Eqs. (4) and (5):

$$\mu_{ep} = \mu_{app1} - \mu_{eo1} = \frac{L_1 \times L_{d1}}{V_1} \times \left(\frac{1}{t_{M1}} - \frac{1}{t_{01}}\right) \quad (4)$$

$$\mu_{ps} = \mu_{app2} - \mu_{eo2} = \frac{L_2 \times L_{d2}}{V_2} \times \left(\frac{1}{t_{M2}} - \frac{1}{t_{02}}\right) \quad (5)$$

where $\mu_{app}$ is apparent mobility, $\mu_{eo}$ is electroosmotic mobility, $L$ = total column length, $L_d$ = the distance between the inlet and the detection point, $V$ = applied voltage, $t_M$ = migration time of solute, $t_0$ = migration time of DMSO, 1 = bare fused-silica column, 2 = modified column. The two values observed in the condition of Fig. 5(B) and the percentages of increase from $\mu_{ep}$ to $\mu_{ps}$ were collected in Table 1. These increases ranging from 2 to 36% indicated that an extra force, besides electrophoretic and electroosmotic forces, drived the solutes toward the detector end of the MAA-CNT capillary and could be regarded as a repulsive chromatography interaction between solutes and modified phases. Differentiating between the electrophoretic and chromatographic contributions to the CEC separation is essential, particularly in this study, which focuses on the chromatographic retention induced by the MWNT. Adopting the definition formulated by Rathore and Horváth, measures of electrophoretic migration and chromatographic retention in CEC can be displayed as a velocity factor ($k_e''$) and a retention factor ($k''$), respectively [56, 57]. In brief, they are expressed by Eqs. (6) and (7)

$$k_e'' = \frac{\mu_{ep}}{\mu_{eo2}} \quad (6)$$

$$k'' = \frac{[t_{M2} \times (1 + k_e'') - t_{02}]}{t_{02}} \quad (7)$$

where $\mu_{eo2}$ is the electroosmotic mobility, which can be obtained from the column 2 as follows:

$$\mu_{eo2} = \frac{L_2 \times L_{d2}}{t_{02} \times V_2} \quad (8)$$

The electrophoretic and chromatographic migration parameters are collected in Table 1. Except for benzamide, data in Table 1 present the negative $\mu_{ep}$ and $k_e''$ values, which means that the electrophoretic migration of solutes was counter to the cathodic EOF in the borate buffer system (pH 8.6, 50 mM). Furthermore, the negative $k''$ values revealed the chromatographic interactions between the analytes and the MAA-CNT phase are repulsive in nature. These results were reasonable when the benzene derivatives were mostly dissociated to anions in the running buffer with a pH level higher than their p$K_a$ values. The anionic analytes did not only electrophoretically move to the anode but also were expelled by the carboxylate groups on the MWNTs.

The migration order of benzene derivatives in Table 1 did not follow either the sequence of $k_e''$ or $k''$ values for the samples. If these values were sorted by groups of aldehydes, ketones, and acids, a negative trend in $k_e''$ and $k''$ values *versus* the order of migration would be found in the group of acids.

 

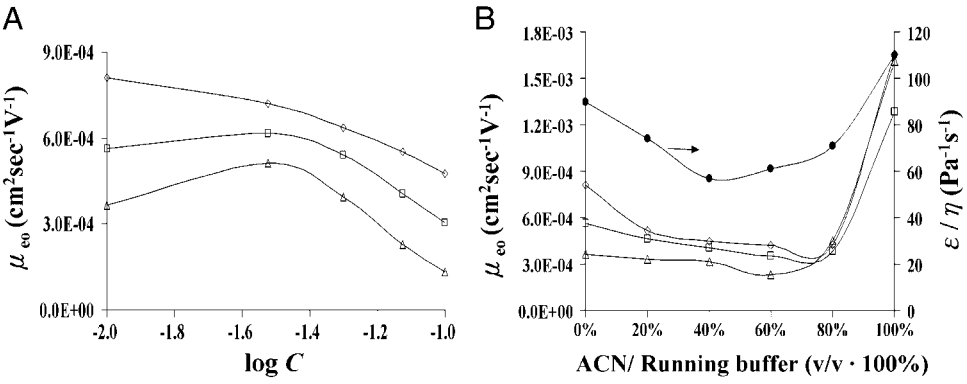


**Figure 4.** Dependence of electroosmotic mobility on phosphate buffer concentration and the percentage of ACN modifier. BGE conditions: phosphate buffer, (A) pH 7.5; (B) 10 mM, pH 7.5. Columns and other conditions are the same as in Fig. 3. (●) denotes the ε/η values of the mixing buffer.

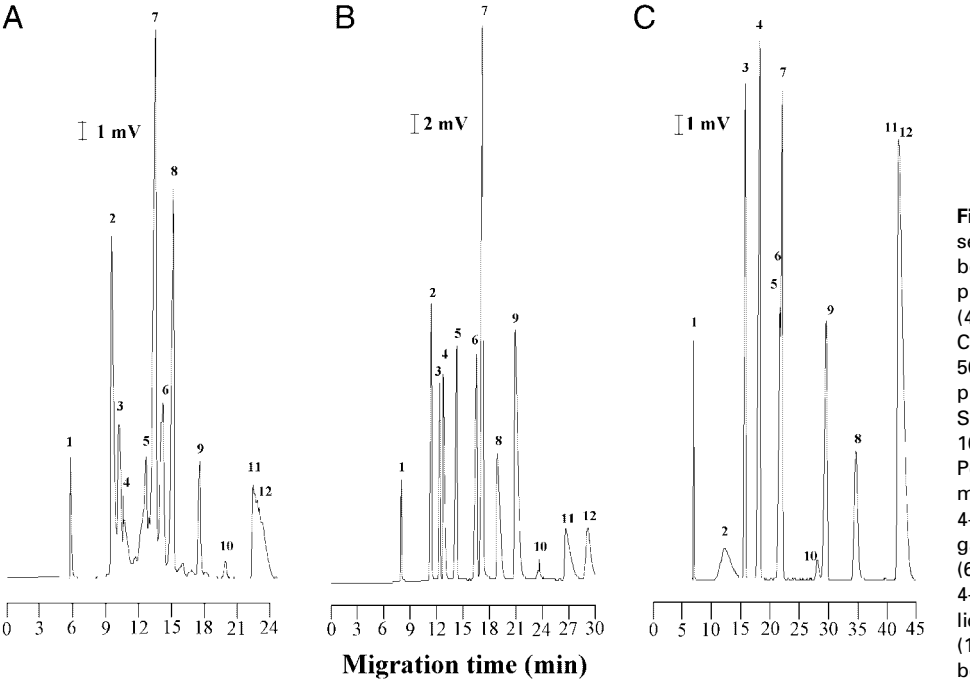


**Figure 5.** Electrochromatographic separations of a mixture of benzene derivatives at different pH values in MAA-CNT capillary (45 cm (41.5 cm) × 75 μm id). Condition: BGE, borate buffer, 50 mM, (A) pH 7.5; (B) pH 8.6; (C) pH 9.5; applied voltage, 10 kV. Samples: hydrostatic injection, 10 cm, 5 s; detection, 214 nm. Peak identification: (1) benzamide; (2) acetovanillone; (3) 4-hydroxyacetophenone; (4) syringaldehyde; (5) acetosyringone; (6) vanillin; (7) syringic acid; (8) 4-hydroxybenzaldehyde; (9) vanillic acid; (10) 4-nitrobenzoic acid; (11) 4-hydroxybenzoic acid; (12) benzoic acid.

The $k_e''$ order indicated an electrophoretic flow proceeded toward the anode for the benzoic acids with higher values, although these $k_e''$ values were very close. On the contrary, the $k''$ value was not consistent with chromatographic retention, which presents high $k''$ values for highly retained solutes. Therefore, electrophoresis predominated over chromatography for the CEC separation of benzoic acids. In contrast, electrophoresis and chromatography collaboratively determined the CEC separation mechanism for the groups of aldehydes and ketones. This would suggest that in addition to the π–π, polar–polar, and electrostatic action, other interactions, such as hydrogen bonding and hydrophobic interactions, might contribute to the chromatographic retention.

### 3.3 Separation of flavonoids

The nine flavonoids exist in many vascular plants and were separated in the previous studies, which included the utilization of silica-hydride monolayer-modified and polyacrylate-modified capillaries [16, 26, 52]. In contrast with benzene derivatives, flavonoids, a less polar class of polyphenols, probably require that some organic modifiers are needed in the running buffer. Neither the hydride-based capillaries, nor the polyacrylate-based capillaries were capable of base-line separations of flavonoids without the addition of MeOH to the buffers. By contrast, the MAA-CNT phase could preliminarily separate the same flavonoids without addition of organic modifier. The role of organic modifier not only altered the EOF, but it also affected the chromatographic partitioning between the flavonoid molecules and the modified capillary surfaces.

After systematic research, the optimum conditions for a separation of select flavonoids in a MEP column suggested a borate buffer, pH 8.8, 150 mM, and an applied voltage of 10 kV. The electrochromatograms demonstrating the effect of the volume ratio of ACN on the separation of these

 

**Table 1.** Electrophoretic properties in the bare fused-silica column and electrochromatographic properties in the MAA-CNT column for the solutes of benzene derivatives, flavonoids and tetracyclines

| Migration order | Solutes | Bare fused-silica column | | MAA-CNT column | | | | |
|---|---|---|---|---|---|---|---|---|
| | | $t_{M1}$ (min) | $\mu_{ep} \times 10^{-4}$ ($cm^2 V^{-1} s^{-1}$)[a] | $t_{M2}$ (min) | $\mu_{ps} \times 10^{-4}$ ($cm^2 V^{-1} s^{-1}$)[a,b] | $k_e''$[c] | $k''$[c] | $N$ ($\times 10^4$)[c] |
| Benzene derivatives separated in the sodium borate buffer (pH 8.6, 50 mM)[d] | | | | | | | | |
| 1 | Benzamide | 4.258 | 0.00 | 8.481 | −0.20 | 0.00 | 0.05 | 9.4 |
| 2 | Acetovanillone | 7.308 | −1.68 | 11.152 | −1.08 (36) | −0.44 | −0.22 | 8.4 |
| 3 | 4-Hydroxyacetophenone | 6.379 | −1.35 | 12.182 | −1.31 (2) | −0.35 | −0.01 | 13 |
| 4 | Syringaldehyde | 7.902 | −1.87 | 12.542 | −1.39 (26) | −0.48 | −0.19 | 6.2 |
| 5 | Acetosyringone | 7.315 | −1.74 | 14.376 | −1.70 (2) | −0.45 | −0.02 | 6.4 |
| 6 | Vanillin | 10.012 | −2.38 | 16.418 | −1.97 (17) | −0.62 | −0.22 | 7.1 |
| 7 | Syringic acid | 10.125 | −2.39 | 17.149 | −2.05 (14) | −0.62 | −0.19 | 8.8 |
| 8 | 4-Hydroxybenzaldehyde | 9.503 | −2.30 | 18.833 | −2.21 (4) | −0.60 | −0.05 | 3.4 |
| 9 | Vanillic acid | 9.942 | −2.38 | 19.132 | −2.24 (6) | −0.62 | −0.09 | 3.4 |
| 10 | 4-Nitrobenzoic acid | 12.333 | −2.71 | 23.128 | −2.52 (7) | −0.70 | −0.14 | 4.9 |
| 11 | 4-Hydroxybenzoic acid | 15.547 | −3.01 | 26.781 | −2.71 (10) | −0.78 | −0.26 | 2.5 |
| 12 | Benzoic acid | 21.98 | −3.37 | 29.136 | −2.80 (17) | −0.87 | −0.54 | 3.3 |
| Flavonoids separated in the borate buffer (pH 8.8, 150 mM) added with ACN (10%, v/v)[e] | | | | | | | | |
| 1 | 5-Methoxyflavone | 7.246 | 1.20 | 4.059 | 2.12 (76) | 0.34 (−0.04) | −0.16 (0.53) | 17 (0.31) |
| 2 | Hesperidin | 7.659 | 1.03 | 4.338 | 1.75 (70) | 0.29 (−0.11) | −0.14 (0.68) | 17 (1.5) |
| 3 | Naringin | 10.127 | 0.32 | 5.407 | 0.70 (119) | 0.09 (−0.07) | −0.10 (0.85) | 47 (2.2) |
| 4 | Daidzein | 10.156 | 0.26 | 5.597 | 0.56 (117) | 0.07 (−0.43) | −0.07 (0.95) | 47 (3.9) |
| 5 | Catechin | 10.367 | 0.20 | 5.754 | 0.45 (129) | 0.05 | −0.06 | 48 |
| 6 | Hesperetin | 10.904 | 0.12 | 5.978 | 0.30 (147) | 0.03 (−0.45) | −0.05 (0.81) | 46 (4.2) |
| 7 | Epicatechin | 11.462 | 0.05 | 6.515 | −0.02 (−139) | 0.01 (−0.38) | 0.02 (0.93) | 17 (1.5) |
| 8 | Naringenin | 12.818 | −0.16 | 7.379 | −0.43 (−169) | −0.05 (−0.46) | 0.09 (0.94) | 31 (3.9) |
| 9 | Quercetin | 14.643 | −0.40 | 8.209 | −0.75 (−88) | −0.11 (−0.46) | 0.12 (4.96) | 25 (160) |
| Tetracyclines separated in the phosphoric acid buffer (pH 2.9, 50 mM)[f] | | | | | | | | |
| 1 | Minocycline | 5.112 | 3.1 | 11.674 | 2.7 (−12) | 1.7 | 1.5 | 5.3 |
| 2 | Chlortetracycline | 5.151 | 3.1 | 18.553 | 2.7 (−14) | 1.7 | 2.9 | 4.0 |
| 3 | Doxycycline | 4.852 | 3.4 | 24.618 | 2.9 (−12) | 1.9 | 4.5 | 6.4 |
| 4 | Tetracycline | 5.636 | 2.7 | 27.552 | 2.3 (−15) | 1.5 | 4.4 | 4.5 |
| 5 | Oxytetracycline | 7.385 | 1.6 | 30.810 | 1.3 (−22) | 0.94 | 3.7 | 7.3 |
| 6 | Methacycline | 8.150 | 1.4 | 31.583 | 1.0 (−26) | 0.77 | 3.4 | 9.2 |
| 7 | Meclocycline | 9.466 | 1.0 | 33.538 | 0.63 (−36) | 0.55 | 3.1 | 5.5 |

a) Observed with an addition of DMSO as an EOF marker in samples.

b) Values in parentheses represent the percentage of increase or decrease from $\mu_{ep}$ to $\mu_{ps}$: $(\mu_{ps}-\mu_{ep}) \times 100\%/\mu_{ep}$.

c) Values in parenthesis are obtained from the BMA-CNT capillary in the borate buffer (pH 9.5, 10 mM) added with ACN (50%, v/v) in [26].

d) CEC conditions are the same as those in Fig. 5(B); a bare fused-silica capillary (60 cm (54.5 cm)) was applied with a voltage of 30 kV; the MAA-CNT capillary (45 cm (41.5 cm)) was applied with a voltage of 10 kV.

e) CEC conditions are the same as those in Fig. 6(C); a bare fused-silica capillary (40 cm (34.5 cm)) was applied with a voltage of 10 kV; the MAA-CNT capillary (40 cm (34.5 cm)) was applied with a voltage of 10 kV.

f) CEC conditions are the same as those in Fig. 8(A); a bare fused-silica capillary (40 cm (35.4 cm)) was applied with a voltage of 10 kV; the MAA-CNT capillary (40 cm (34.5 cm)) was applied with a voltage of 10 kV.

flavonoids in the BMA-MES capillary are given in Fig. 6. Their migration times, moreover, increased with an increase in the modifier percentages. Without a doubt, this happened because the organic modifier decreased the EOF, as a result of a reduction in the value of $\varepsilon/\eta$, as shown in Fig. 4(B). Among the four ratios of ACN tried, the 10% solution clearly achieved the best resolution of the flavonoids, as shown in Fig. 6(C), where the electrochromatographic parameters are also listed in Table 1. Other conditions based on the 10% ACN addition were also tried, for example, changing the pH level (pH 8.3 and pH 9.3) and buffer concentration (100 and 200 mM). However, the separation performances under these trial conditions of running bufers were still not comparable to Fig. 6(C).

In Table 1, the first six eluted compounds had the $\mu_{ps}$ values larger than their corresponding $\mu_{ep}$ values, and thus

 

had negative $k''$ values as in the case of the separation of benzene derivatives. On the contrary, smaller $\mu_{ps}$ values and positive $k''$ values were observed for the last three eluted compounds. Both the $k_e''$ and $k''$ values are totally parallel to the migration order of flavonoids, that is, the electrophoretic and chromatographic mode collaboratively determined the CEC mechanism. Data in Table 1 also present the flavonoids have higher $k''$ values than the benzene derivatives. This could be due to the increased number of benzene rings existing in the flavonoid structure and exerting stronger π–π interactions, as well as Van der Waals forces. However, these $k''$ values are lower than the parenthetic values obtained from the BMA-CNT capillary in a borate buffer with high volume percentage of ACN modifier (50%). The hydrophilic polyacrylamide network in the MAA-CNT phase would prevent the less polar flavonoids from approaching the phase and cause a lower column efficiency, represented by $N$ values, than that observed in the BMA-CNT capillary.

Small differences in the skeleton or a different substituent position on the flavonoid compounds may cause variation in the retention time in an RP LC mode [58]. In this mode, the values of $k''$ would be decreased as organic modifier was increased. As shown in Fig. 7, however, the plots of $k''$ values against the ACN volume ratios present convave curves with maxima around 10% ACN. This phenomenon could be contributed by the increase in $pK_a$ values of these flavonoids as the ACN began to be added in the running buffer, and then more neutral solutes were formed and retained [59].

### 3.4 Separation of tetracyclines

TC antibiotics have been widely used as veterinary medicine and their residues in edible products are often determined. In a previous study, four prepared TCs could not be well resolved by the SiH-CNT2 capillary but the separation could be improved by increasing the quantity of MWNTs moieties attached to the stationary phase [25]. The BMA-CNT capillary was also tried to separate the TCs in various buffer conditions, but peaks were still unresolved. Based on the CNTs immobilized phases, the separation resolution of TCs could be greatly determined by the phase matrix. Increasing the polarity of TCs by protonation or deprotonation could be a good strategy to separate them in the MAA-CNT capillary.

In this study, the MAA-CNT capillary could accommodate enough MWNT units copolymerized on the hydrophilic polyacrylamide bonded phase to achieve satisfactory separations of seven TCs, the structures of which are presented in Fig. 1, under the acidic buffer conditions of phosphate and acetate solutions, as shown in Figs. 8(A) and (B), respectively. The two buffer conditions were optimized by varying pH and concentration, and were carefully checking the corresponding electrochromatograms. Citrate buffers were also tried but only achieved poor resolution of the TCs, as shown in Fig. 8(C). Here, the citrate molecules might be adsorbed on the MWNTs through van der Waals force and the interaction with metallic impurity, such as Fe catalyst for the systhesis of MWNTs [60, 61]. The adsorption affected the retention of TCs on the MWNTs and induced the distortion of some peaks. This phenomenon is prominent after 30 min of electroseparation but not serious for the

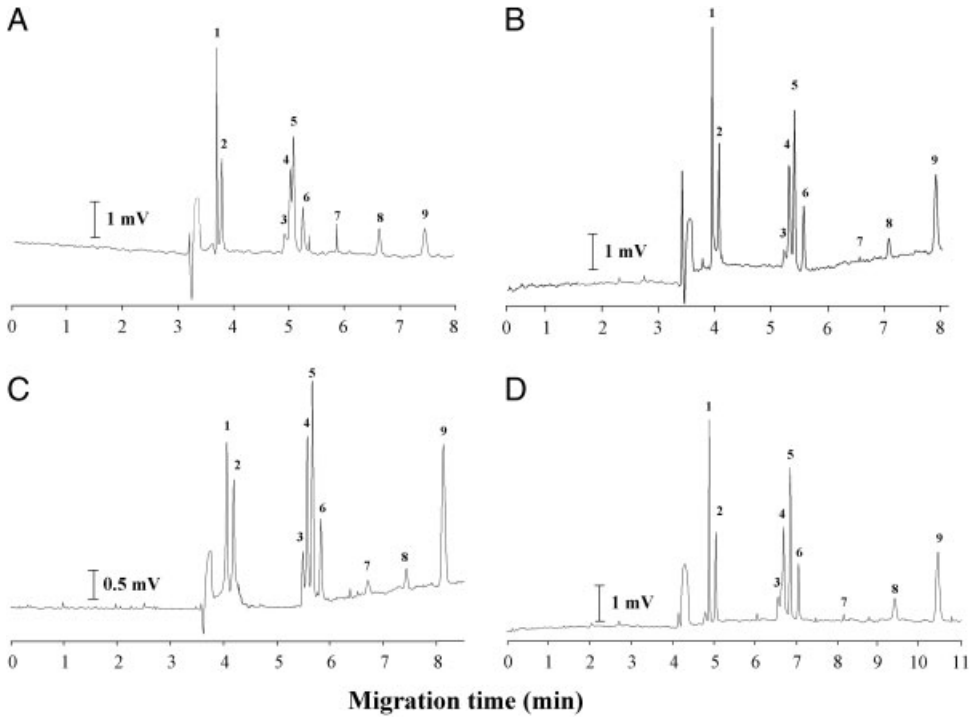


**Figure 6.** Electrochromatographic separations of flavonoids in MAA-CNT capillary (40 cm (34.5 cm) × 75 μm id) at various volume ratios of ACN added in BGE. (A) 0%; (B) 5%; (C) 10%; (D) 15% of ACN added in borate buffer, 150 mM, pH 8.8. Applied voltage: 10 kV. Samples: hydrostatic injection, 10 cm, 5 s; detection, 280 nm. Peak identification: (1) 5-methoxyflavone, (2) hesperidin, (3) naringin, (4) daidzein, (5) catechin, (6) hesperetin, (7) epicatechin, (8) naringenin, (9) quercetin.

 

phosphate and acetate buffers. In comparison with Fig. 8(A), the electrochromatogram of Fig. 8(D) observed on the bare fused-silica column shows poor resolution but high separation efficiency, while the band broadening coming from the chromatographic retention was not included.

Some peaks split from peak 1 (MNC) and peak 2 (CTC) could be found in Fig. 8 and assigned as peaks 1′, 2′, and 2″. Sample TCs would undergo degradation to complex mixtures because of their sensitivity to acids, bases, and heat [62]. When TCs were exposed to dilute acids, anhydrotetracyclines were formed by dehydration and they could rearrange at C-4 position to form α- and β-apoterramycin stereoisomers [63, 64]. Accordingly, the split peaks might be regarded as the anhydrotetracycline or apoterramycin derivatives of MNC and CTC. In contrast to reactions in acidic media, in alkaline media, an isotetracycline derivative with a γ-lactone structure was formed and separated from the other TCs in the previous study [25].

Table 1 shows the electrochromatographic properties of TCs migrating in the phosphate buffer conditions of Fig. 8(A). Here, all the TCs solutes bore positive values of effective charge on the tertiary amine substituents in the pH 2.9 medium (MNC: $pK_a = 2.8, 5.0, 7.8, 9.5$ for $H_4A^{+2}$; CTC: $pK_a = 3.33, 7.55, 9.33$ for $H_3A^{+}$; doxycycline: $pK_a = 3.02$,

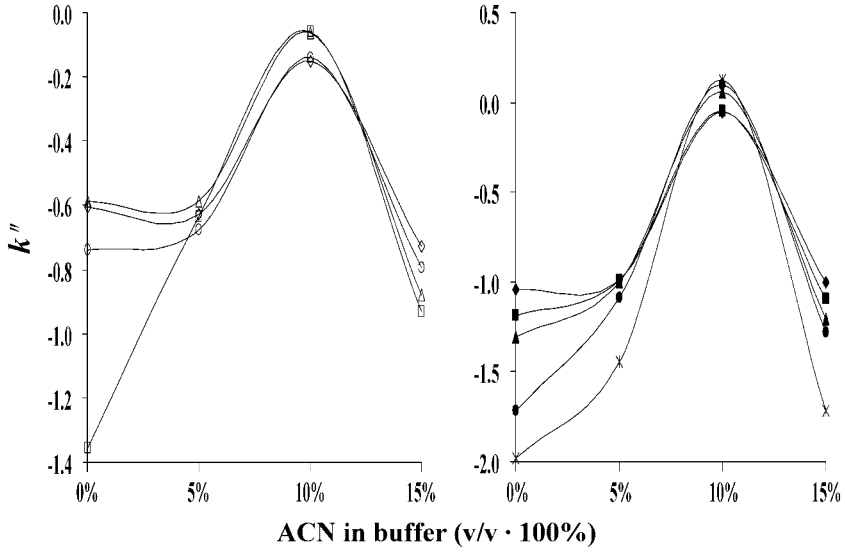


**Figure 7.** Effect of the addition of ACN to the running buffer on the retention factor, $k''$ of flavonoids in the MAA-CNT capillary. CEC conditions and data are based on those in Fig. 6. Data: (◇) 5-methoxyflavone, (○) hesperidin, (Δ) naringin, (□) daidzein, (♦) catechin, (■) hesperetin, (▲) epicatechin, (●) naringenin, (×) quercetin.

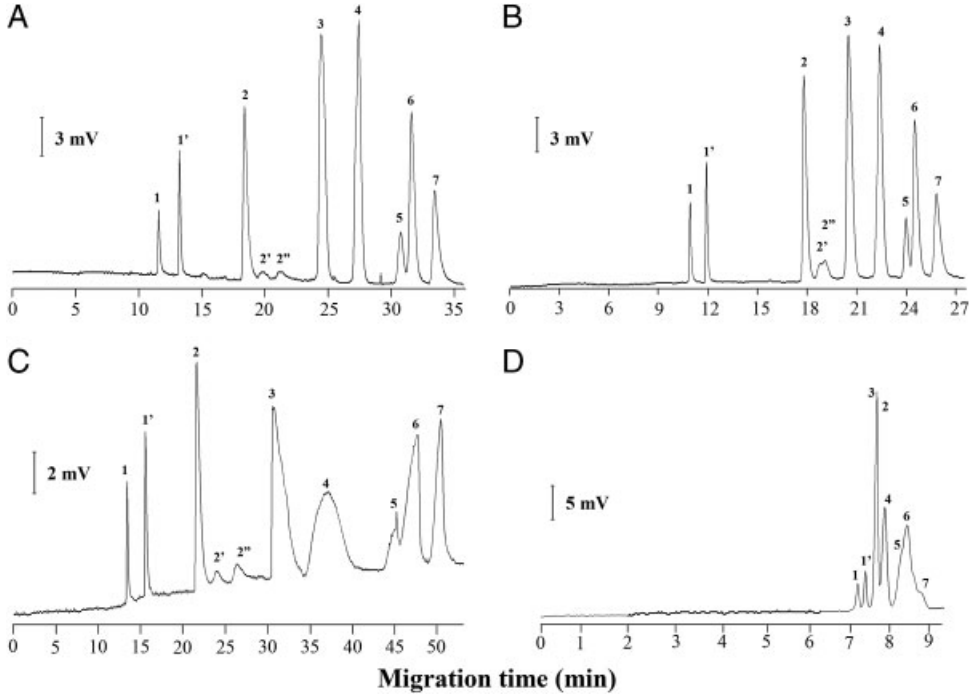


**Figure 8.** Electrochromatographic separations of TCs at different buffers in the MAA-CNT and the bare fused-silica capillaries (40 cm (34.5 cm) × 75 μm id). BGE: (A) pH 2.9 in phosphate buffer, 50 mM; (B) pH 2.3 in acetate buffer, 50 mM; (C) pH 2.9 in citrate buffer, 50 mM. (A), (B), and (C) were observed on the MAA-CNT capillary, but (D) was observed on the bare fused-silica capillary with the BGE (A). Applied voltage: 10 kV. Samples: hydrostatic injection, 10 cm, 5 s; detection, 355 nm. Peak identification is shown in Fig. 1. Peaks (1′), (2′), and (2″) are derivatives of MNC (1) and CTC (2).

 

7.97, 9.15 for $H_3A^+$; TC: $pK_a = 3.32$, 7.78, 9.58 for $H_3A^+$; oxytetracycline: $pK_a = 3.32$, 7.46, 8.94 for $H_3A^+$; methacycline: $pK_a = 3.5$, 7.6, 9.2 for $H_3A^+$; meclocycline: $pK_a = 4.05$, 6.87, 9.59 for $H_3A^+$ [65–67]) and exhibited positive $\mu_{ep}$ values. The $\mu_{ps}$ values were also positive, but were smaller than $\mu_{ep}$ values. There should exist chromatographic retentions of the TCs with positive $k''$ values. In comparison with the other $k''$ values in Table 1, the greater $k''$ of the TCs solutes may greatly result from the electrostatic interactions between positively charged TCs and negatively charged MWNTs. The chromatographic contribution to the migration order is obviously found in the first three eluted TCs, whereas the electrophoresis primarily determined the order for the last four TCs.

## 4 Concluding remarks

Comparison of ATR-IR and EOF profiles, which were recorded for capillaries synthesized from the *in situ* polymerization with acid-treated MWNTs and from the stepwise incorporation of MWNTs on silica-hydride phase, proved that the new stationary phase, MAA-CNT, was successfully bonded on the capillary wall, and the new phase exhibited great potential for application in OT-CEC due to its unique surface functionality. Three prepared samples with various polarity and dissociation properties were used to evaluate the extent of electrophoretic and chromatographic contributions to the CEC mechanism. The sample of benzene derivatives was well separated when the anioic solutes electrophoretically migrated to the anode and were simultaneously repulsed by the carboxylate groups on the MWNTs. Among them, the electrophoretic discrimination between benzoic acids determined the migration order. Flavonoids, with less polarity, were more subject to chromatographic retention, resulting from π–π interactions, hydrogen bonding and hydrophobic interactions with the BMA-CNT capillary in comparison with the MAA-CNT capillary. For TCs, their migration rates were mainly controlled by the cathodic electrophoretic flow or by electrostatic attractions with the carboxylated MWNTs, and their separation resolutions were greatly influenced by the phase matrix effect.

*Support of this work by the National Science Council of Taiwan (NSC-98-2113-M-039-003-MY3) and China Medical University (CMU99-S-48) is gratefully acknowledged.*

*The authors have declared no conflict of interest.*

## 5 References

[1] Ou, J., Dong, J., Dong, X., Yu, Z., Ye, M., Zou, H., *Electrophoresis* 2007, *28*, 148–163.

[2] Dong, X., Wu, R., Dong, J., Wu, M., Zhu, Y., Zou, H., *Electrophoresis* 2009, *30*, 141–154.

[3] Pesek, J. J., Matyska, M. T., Salgotra, V., *Electrophoresis* 2008, *29*, 3842–3849.

[4] Yin, X.-B., Liu, D.-Y., *J. Chromatogr. A* 2008, *1212*, 130–136.

[5] Xu, L., Dong, X. Y., Sun, Y., *Electrophoresis* 2009, *30*, 689–695.

[6] Huang, X., Zhang, J., Horváth, Cs., *J. Chromatogr. A* 1999, *858*, 91–101.

[7] Chuang, S.-C., Chang, C.-Y., Liu, C.-Y., *J. Chromatogr. A* 2004, *1044*, 229–236.

[8] Tan, Z. J., Remcho, V. T., *Anal. Chem.* 1997, *69*, 581–586.

[9] Huang, T., Mi, J.-Q., Zhang, X.-X., *J. Sep. Sci.* 2006, *29*, 277–281.

[10] Eeltink, S., Svec, F., Fréchet, J. M. J., *Electrophoresis* 2006, *27*, 4249–4256.

[11] Xu, L., Sun, Y., *Electrophoresis* 2007, *28*, 1658–1667.

[12] Xu, L., Sun, Y., *Electrophoresis* 2008, *29*, 880–888.

[13] Xu, L., Sun, Y., *J. Chromatogr. A* 2008, *1183*, 129–134.

[14] Zaidi, S. A., Cheong, W. J., *J. Chromatogr. A* 2009, *1216*, 2947–2952.

[15] Xu, L., Dong, X.-Y., Sun, Y., *Electrophoresis* 2009, *30*, 689–695.

[16] Chen, J.-L., Lin, Y.-C., *J. Chromatogr. A* 2010, *1217*, 4328–4336.

[17] Smith, N. W., Jiang, Z., *J. Chromatogr. A* 2008, *1184*, 416–440.

[18] Nilsson, C., Birnbaum, S., Nilsson, S., *J. Chromatogr. A* 2007, *1168*, 212–224.

[19] Dong, X. L., Wu, R. A., Wu, M. H., Dong, J., Wu, M., Zhuz, Y., Zou, H., *Electrophoresis* 2008, *29*, 3933–3940.

[20] Hsieh, Y. L., Chen, T. H., Liu, C. P., Liu, C. Y., *Electrophoresis* 2005, *26*, 4089–4097.

[21] Li, T., Xu, Y., Feng, Y.-Q., *J. Liq. Chromatogr. Rel. Technol.* 2009, *32*, 2484–2498.

[22] Yang, L., Guihen, E., Holmes, J. D., Loughran, M., O'Sullivan, G. P., Glennon, J. D., *Anal. Chem.* 2005, *77*, 1840–1846.

[23] Li, H.-F., Zeng, H., Chen, Z., Lin, J.-M., *Electrophoresis* 2009, *30*, 1022–1029.

[24] Sombra, L., Moliner-Martínez, Y., Cárdenas, S., Valcárcel, M., *Electrophoresis* 2008, *29*, 3850–3857.

[25] Chen, J.-L., *J. Chromatogr. A* 2010, *1217*, 715–721.

[26] Chen, J.-L., Lu, T.-L., Lin, Y.-C., *Electrophoresis* 2010, *31*, 3217–3226.

[27] Jia, Z., Wang, Z., Xu, C., Liang, J., Wei, B., Wu, D., Zhu, S., *Mater. Sci. Eng.* 1999, *271*, 395–400.

[28] Park, S. J., Cho, M. S., Lim, S. T., Choi, H. J., Jhon, M. S., *Macromol. Rapid Commun.* 2003, *24*, 1070–1073.

[29] Jiang, Z., Smith, N. W., Ferguson, P. D., Taylor, M. R., *Anal. Chem.* 2007, *79*, 1243–1250.

[30] Guryča, V., Mechref, Y., Palm, A. K., Michálek, J., Pacáková, V., Novotný, M. V., *J. Biochem. Biophys. Methods* 2007, *70*, 3–13.

[31] Dong, X., Wu, R., Dong, J., Wu, M., Zhu, Y., Zou, H., *Electrophoresis* 2008, *29*, 919–927.

 

[32] Silverstein, R. M., Webster, F. X., Kiemle, D., *Spectrometric Identification of Organic Compounds*, 7th Edn, Wiley, NJ 2005.

[33] Kang, X., Ma, W., Zhang, H.-L., Xu, Z.-G., Guo, Y., Xiong, Y., *J. Appl. Polym. Sci.* 2008, *110*, 1915–1920.

[34] Zou, W., Du, Z., Liu, Y., Yang, X., Li, H., Zhang, C., *Compos. Sci. Technol.* 2008, *68*, 3259–3264.

[35] Liu, J., Rinzler, A. G., Dai, H., Hafner, H., Bradley, R. K., Boul, P. J., Lu, A., Iverson, T., Shelimov, K., Huffman, C. B., Rodriguez-Macias, F., Shon, Y., Lee, T. R., Colbert, D. T., Smalley, R. E., *Science* 1998, *280*, 1253–1256.

[36] Jankowska, H., Swiatkowski, A., Choma, J., *Active Carbon*, Ellis Horwood Ltd., New York 1991.

[37] Clayden, J., Greeves, N., Warren, S., Wothers, P., *Organic Chemistry*, Oxford University Press, New York 2001.

[38] Hjertén, S., *J. Chromatogr.* 1985, *347*, 191–198.

[39] Cobb, K. A., Dolnik, V., Novotny, M., *Anal. Chem.* 1990, *62*, 2478–2483.

[40] Lu, M., Zhang, L., Lu, Q., Chi, Y., Chen, G., *Electrophoresis* 2009, *30*, 2273–2279.

[41] Chen, X. H., Chen, C.-S., Chen, Q., Cheng, F.-Q., Zhang, G., Chen, Z.-Z., *Mater. Lett.* 2002, *57*, 734–738.

[42] Smoluchowski, M. v., *Handbuch der Elektrizität und des Magnetismus*, Barth, Liepzig 1921.

[43] Rice, C., Whitehead, R., *J. Phys. Chem.* 1965, *69*, 4017–4024.

[44] Hiemenz, P. C., Rajagopalan, R., *Principles of Colloid and Surface Chemistry*, Marcel Dekker, New York 1997.

[45] Rathore, A. S., Wen, E., Horváth, Cs., *Anal. Chem.* 1999, *71*, 2633–2641.

[46] Lyklema, J., Minor, M., *Colloids Surf. A Physicochem. Eng. Asp.* 1998, *140*, 33–41.

[47] Choudhary, G., Horvath, Cs., *J. Chromatogr. A* 1997, *781*, 161–183.

[48] Knox, J. H., Grant, I. H., *Chromatographia* 1991, *32*, 317–318.

[49] Huang, X., Zhang, J., Horvath, Cs., *J. Chromatogr. A* 1999, *858*, 91–101.

[50] Chen, G., Tallarek, U., Seidel-Morgenstern, A., Zhang, Y., *J. Chromatogr. A* 2004, *1044*, 287–294.

[51] Chen, J.-L., *Electrophoresis* 2009, *30*, 3855–3862.

[52] Chen, J.-L., *J. Chromatogr. A* 2009, *1216*, 6236–6244.

[53] Chen, J.-L., *Electrophoresis* 2006, *27*, 729–735.

[54] Lobbes, J. M., Fitznar, H. P., Kattner, G., *Anal. Chem.* 1999, *71*, 3008–3012.

[55] Chen, M.-Y., Chang, Y. -Z., Lu, F.-J., Chen, J.-L., *Anal. Sci.* 2010, *26*, 561–567.

[56] Rathore, A. S., Horváth, Cs., *J. Chromatogr. A* 1996, *743*, 231–246.

[57] Rathore, A. S., Horváth, Cs., *Electrophoresis* 2002, *23*, 1211–1216.

[58] Wang, S. P., Fu, M. D., Wang, M. H., *J. Chromatogr. A* 2007, *1164*, 306–312.

[59] Porras, S. P., Kenndler, E., *J. Chromatogr. A* 2004, *1037*, 455–465.

[60] Lindegren, M., Loring, J. S., Persson, P., *Langmuir* 2009, *25*, 10639–10647.

[61] McKee, G. S. B., Deck, C. P., Vecchio, K. S., *Carbon* 2009, *47*, 2085–2094.

[62] Barton, D. H. R., Magnus, P. D., *J. Chem. Soc. C* 1971, 2164–2166.

[63] Hochstein, F. A., Stephens, C. R., Gordon, P. N., Regna, P. P., Pilgrim, F. J., Brunings, K. J., Woodward, R. B., *J. Am. Chem. Soc.* 1952, *74*, 3707–3708.

[64] Sina, A., Youssef, M. K., Kassems, A. A., Attia, I. A., *J. Pharm. Sci.* 1971, *60*, 1544–1547.

[65] Butterfield, A. G., Hughes, D. W., Pound, N. J., Wilson, W. L., *Antimicrob. Agents Chemother.* 1973, *4*, 11–15.

[66] Qiang, Z., Adams, C., *Water Res.* 2004, *38*, 2874–2890.

[67] Avery, G. S., in: *Drug Treatment Principles and Practice of Clinical Pharmacology and Therapeutics*, 2nd Edn, Adis Press, Sydney 1980.

 